

1009

1010 **Supplementary Fig. 1 Cryo-EM data collection, image processing, model building, and**

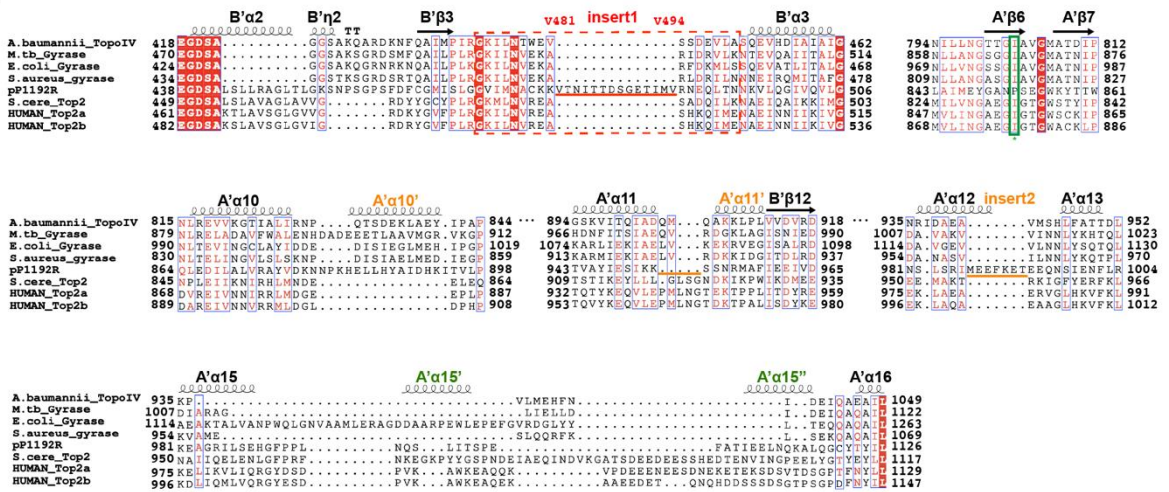
1011 **refinement.** (A) Representative cryo-EM image with apo pP1192R particles are highlighted by

1012 green circles. Scale bar represents 20 nm. (B) Reference-free 2D classification. (C) Flow chart

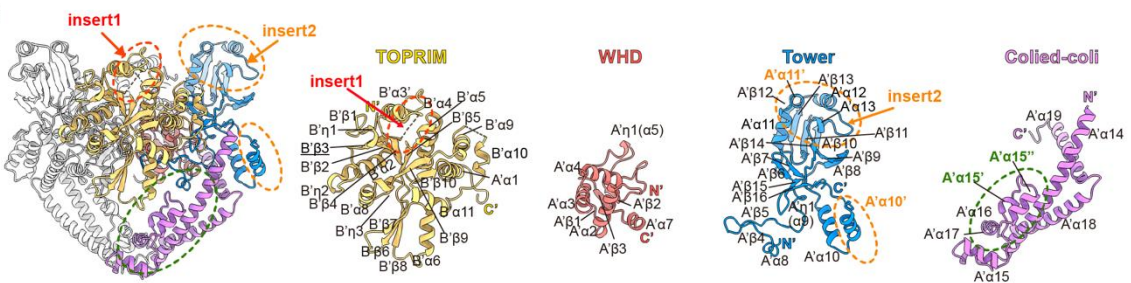
1013 of the cryo-EM data processing. Details can be found in Materials and Methods. (D) Local

1014 resolution for the DNA-binding/cleavage domain in the closed state and open state. (E and F)
1015 Golden Standard Fourier Shell Correlation (GSFSC) curve for the DNA-binding/cleavage
1016 domain in the closed state (E) and open state (F). (G and H) Euler angle distribution for the
1017 DNA-binding/cleavage domain in the closed state (G) and open state (H).
1018

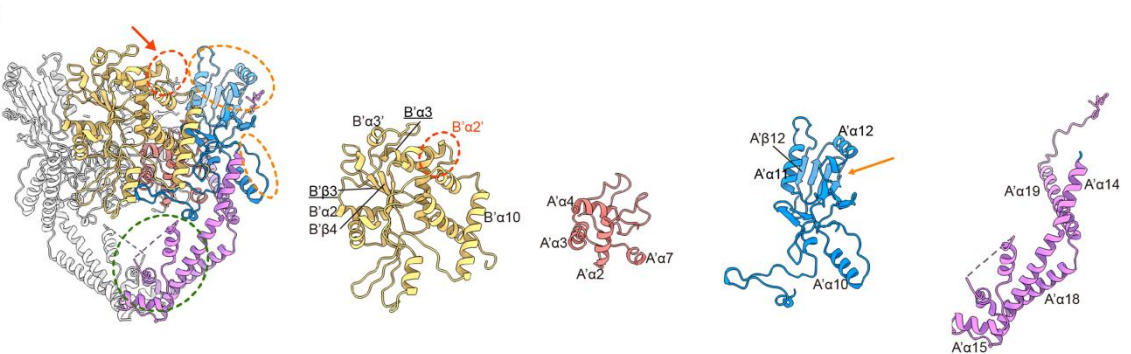
A



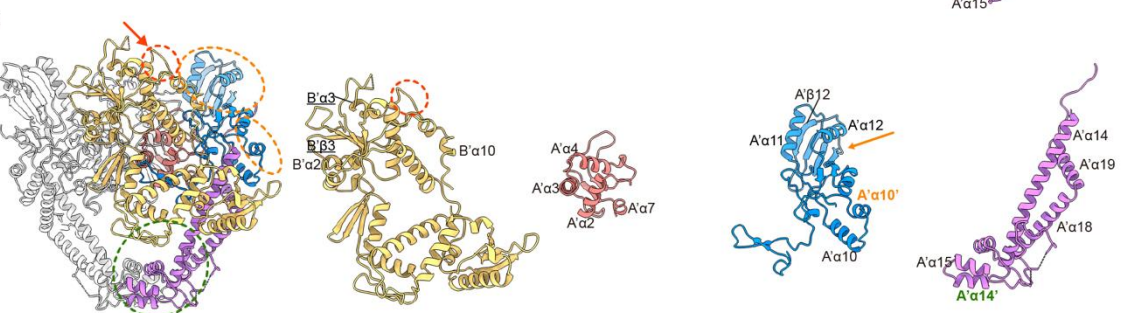
B



C



D



1019

1020

Supplementary Fig. 2 Structural details of the DNA binding/cleavage domain in pP1192R.

1021

(A) Structure-based sequence alignment of pP1192R DNA binding/cleavage domain with other

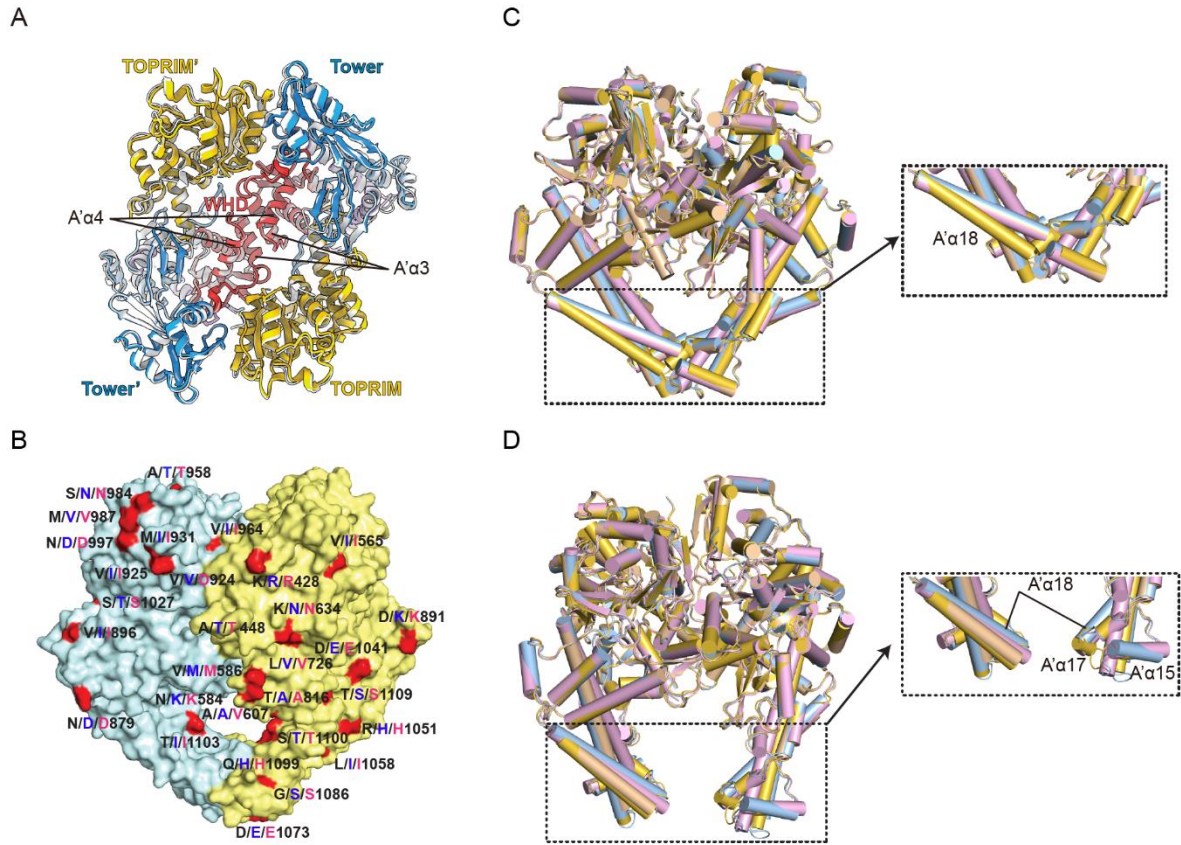
1022

Topo IIAs homologs. Secondary structural elements of pP1192R are indicated above the

1023

sequence alignment. Underline sequences of insert1 and insert2 in red and yellow. G471-N501

1024 is emphasized with a red box. P852 is highlighted with a green box, and an asterisk is noted
1025 below the sequence. (B-D) Cartoon representations the closed-state dimers and individual
1026 domains of Topo IIAs. In each structural representation, individual domains of ASFV pP1192R
1027 (B), human Topo II α (C), and *E.coli* gyrase (D) are colored as in Fig. 1D.
1028



1029

1030 **Supplementary Fig. 3 Comparison between the open and closed states of pP1192R.** (A)

1031 Structural superimposition of apo pP1192R in the open state (white) and close state (colored as

1032 shown in Fig. 1D). (B) The surface presentation of the DNA binding/cleavage core highlights

1033 differing amino acids (shown in red) between ASFV strains. Amino acids of pP1192R from the

1034 current ASFV strain (GenBank: AXB50031.1) are labeled in black, while those from strain

1035 Georgia07 or strain L60 are shown in blue and purple respectively. One protomer is cyan and

1036 the other is yellow. (C and D) Structural superimposition of the closed (C) and open states (D)

1037 of the current pP1192R (gold) with those of strain Georgia07 (pink) and strain L60 (conformers

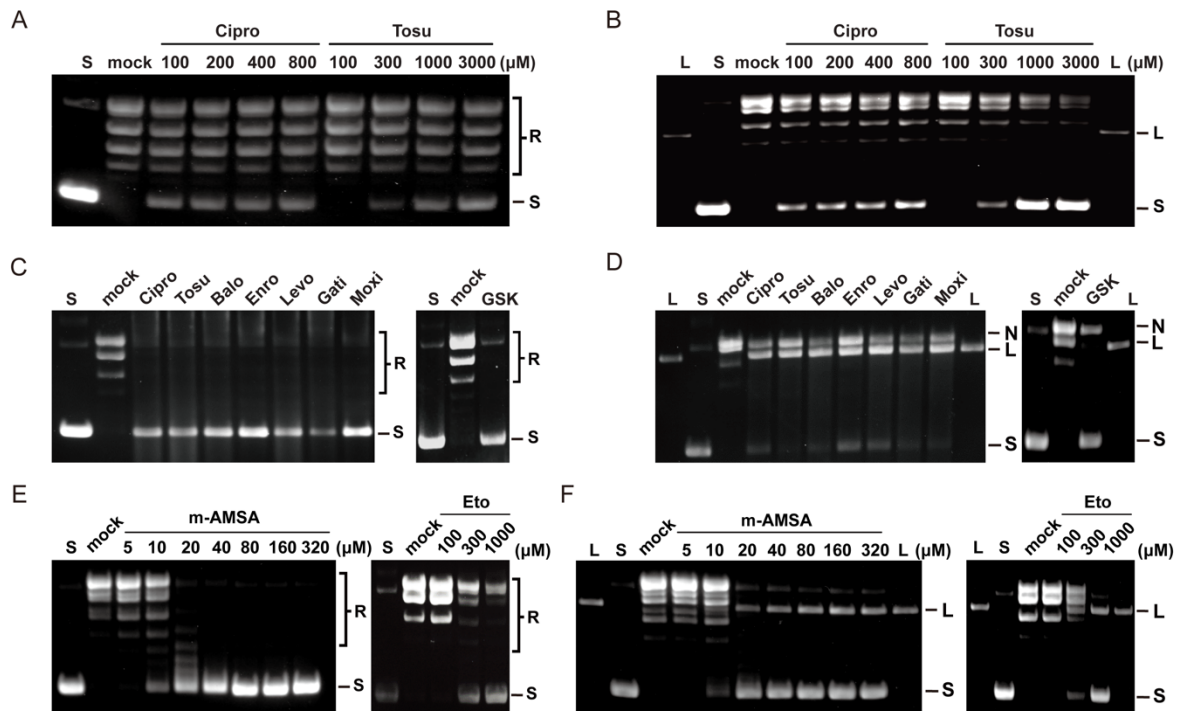
1038 IIa and IIIa shown in cyan, conformers IIb and IIIb shown in wheat). Structural variations in

1039 the closed states are mainly focused on the C-gate, highlighted by a conformational fine-tuning

1040 A' α 18, while differences in the open states are observed at A' α 15, A' α 17 and A' α 18.

1041

1042



1043

1044 **Supplementary Fig. 4 Evaluation of antibacterial and anticancer drugs against Topo IIs.**

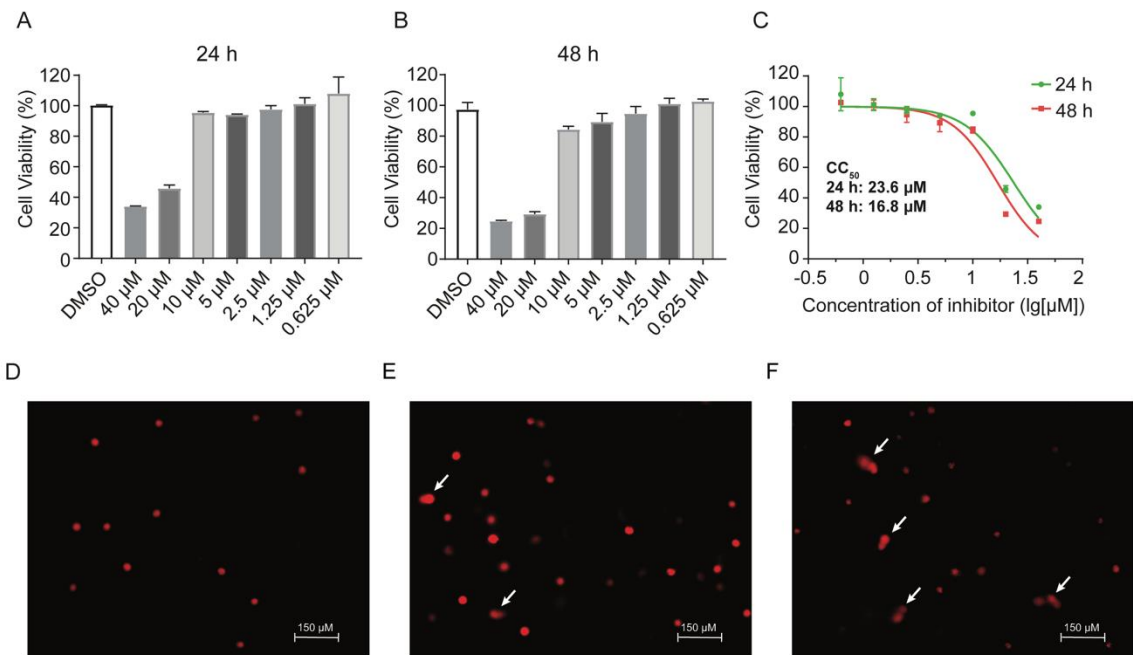
1045 (A and B) Inhibition of ciprofloxacin (Cipro) and tosofloxacin (Tosu) against pP1192R
 1046 evaluated by relaxation assays (A) and cleavage assays (B). Drugs were tested at serial dilutions
 1047 (final concentrations shown) starting from their respective highest concentration without drug
 1048 precipitation. S, R and L represent the supercoiled, relaxed and linear DNA bands, respectively.

1049 (C and D) Inhibition of fluoroquinolones and GSK299423 against *Acinetobacter baumannii*
 1050 topoisomerase IV evaluated by relaxation assays (C) and cleavage assays (D). The antibacterial
 1051 drugs were all tested at a final concentration of 2 μ M. The gel shows that fluoroquinolones can
 1052 induce both single-stranded (linear DNA band) and double-stranded (nicked DNA band) DNA
 1053 breaks, whereas GSK induces only single-stranded DNA break (linear DNA band). S, R and L
 1054 represent the supercoiled, relaxed and linear DNA products, respectively.

1055 (E and F) Inhibition of anticancer drugs against human Topo II α evaluated by relaxation assays (E) and cleavage
 1056 assays (F). The final concentrations of drugs are shown. M-AMSA and etoposide induce only
 1057 increasing linear products with increasing drug concentration in human Topo II α , while the
 1058 nicked DNA bands were at the same level as those shown in the pUC19 plasmid substrate.

1059 Linear (L), nicked (N), relaxed (R), and supercoiled (S) forms of DNA are labelled.

1060



1061

1062 **Supplementary Fig. 5 The influence of m-AMSA on the viability of PAM cells.** (A and B)

1063 Assessment of m-AMSA cytotoxicity in PAM cells after 24 h (A) or 48 h (B) of m-AMSA

1064 treatment using the CCK-8 assay. (C) Calculation of CC₅₀ using nonlinear regression analysis.

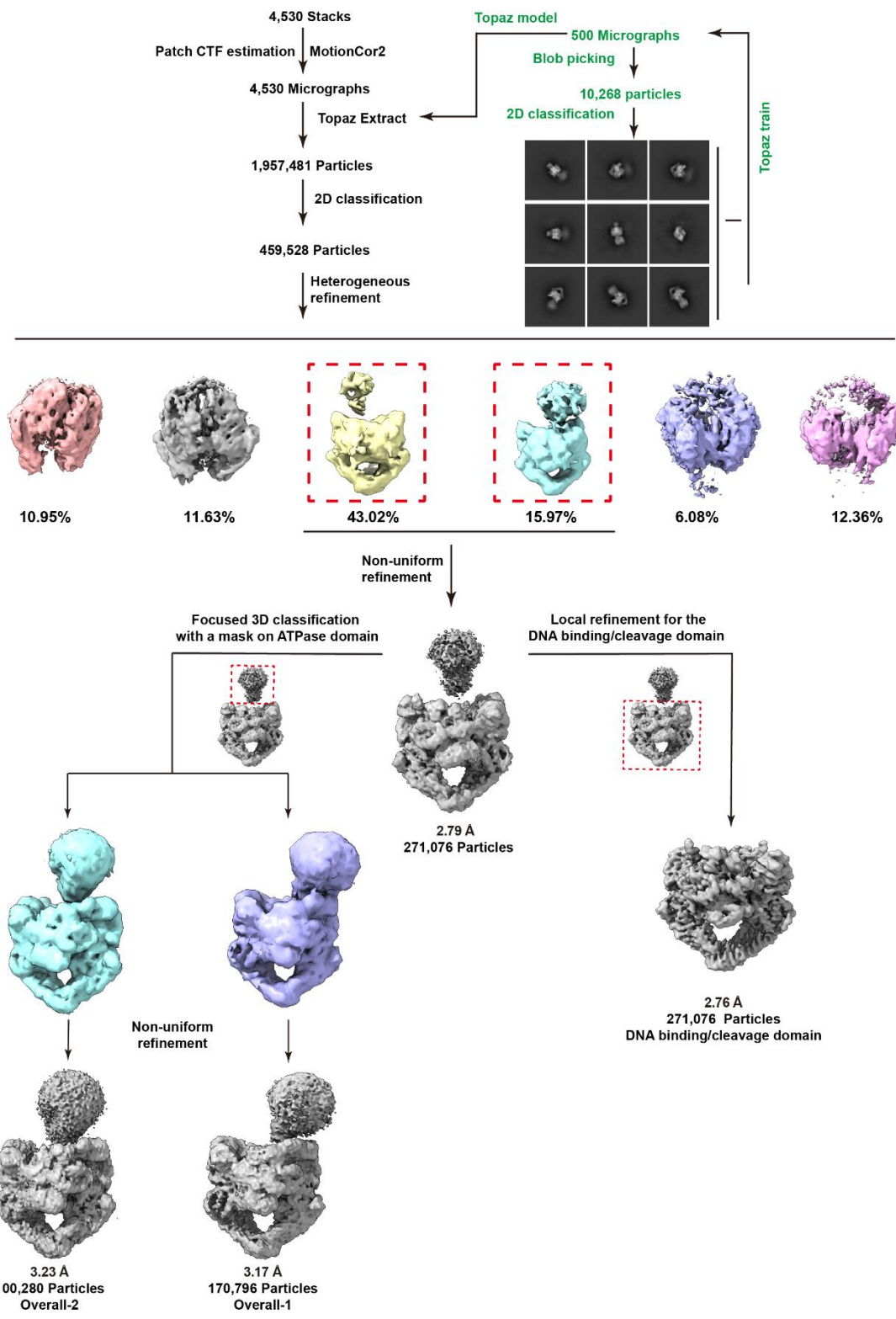
1065 (D-F) Comet assay analysis of DNA damage in the PAM cells infected with ASFV and not

1066 exposed to m-AMSA (D), non-infected and exposed to m-AMSA (E), and infected and exposed

1067 to m-AMSA (F). The scale bar in the fluorescence images is 150 μm.

1068

1069

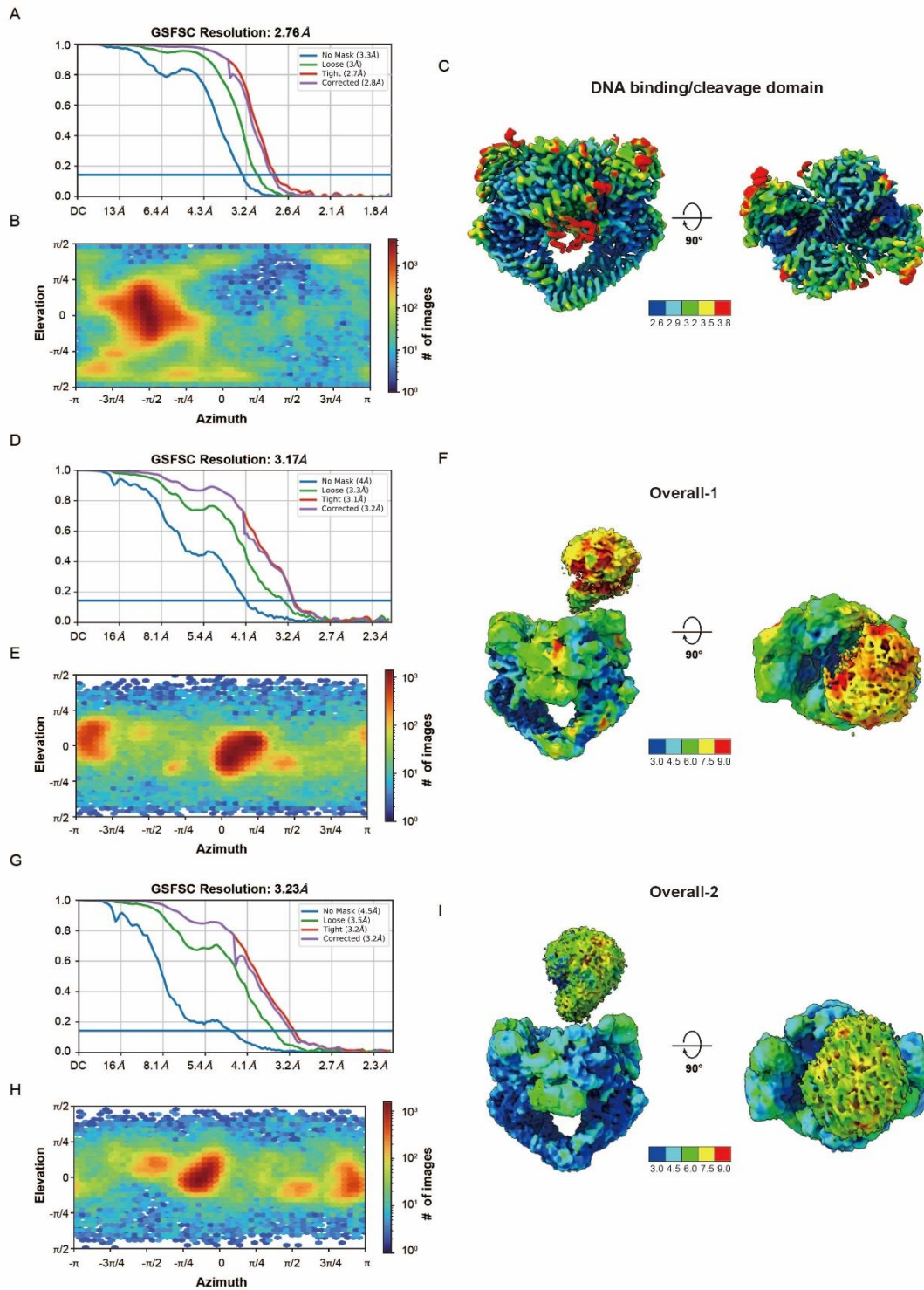


1070

1071 **Supplementary Fig. 6 Flowchart of cryo-EM data collection, image processing, model**

1072 **building, and refinement.** Please refer to the ‘Image Processing’ in Methods section for details.

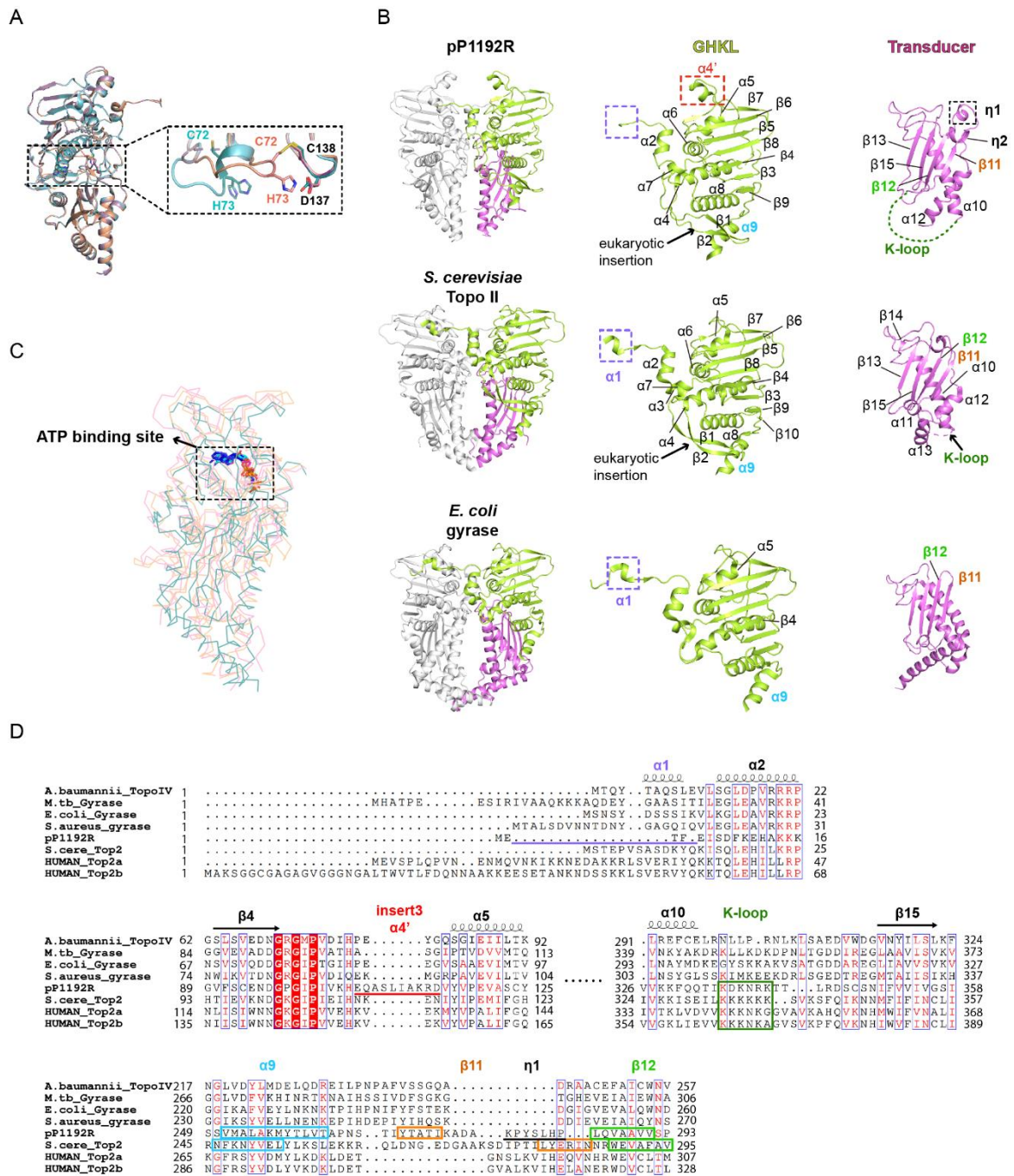
1073



1074

1075 **Supplementary Fig. 7 Structural data validation and local resolution.** The Fourier Shell
 1076 Correlation (FSC) plot and resolution estimation using the gold-standard 0.143 criterion (A, D,
 1077 G). Particle angular distribution plots (B, E, H). Local resolution for the DNA-binding/cleavage
 1078 domain in pP1192R-DNA-m-AMSA complex (C) and for the overall-1 (F) and overall-2 (I).

1079



1080

1081 **Supplementary Fig. 8 Structural details of the pP1192R ATPase domain. (A)**

1082 Superimposition of ATPase domains in the present pP1192R (purple) with those in the reduced

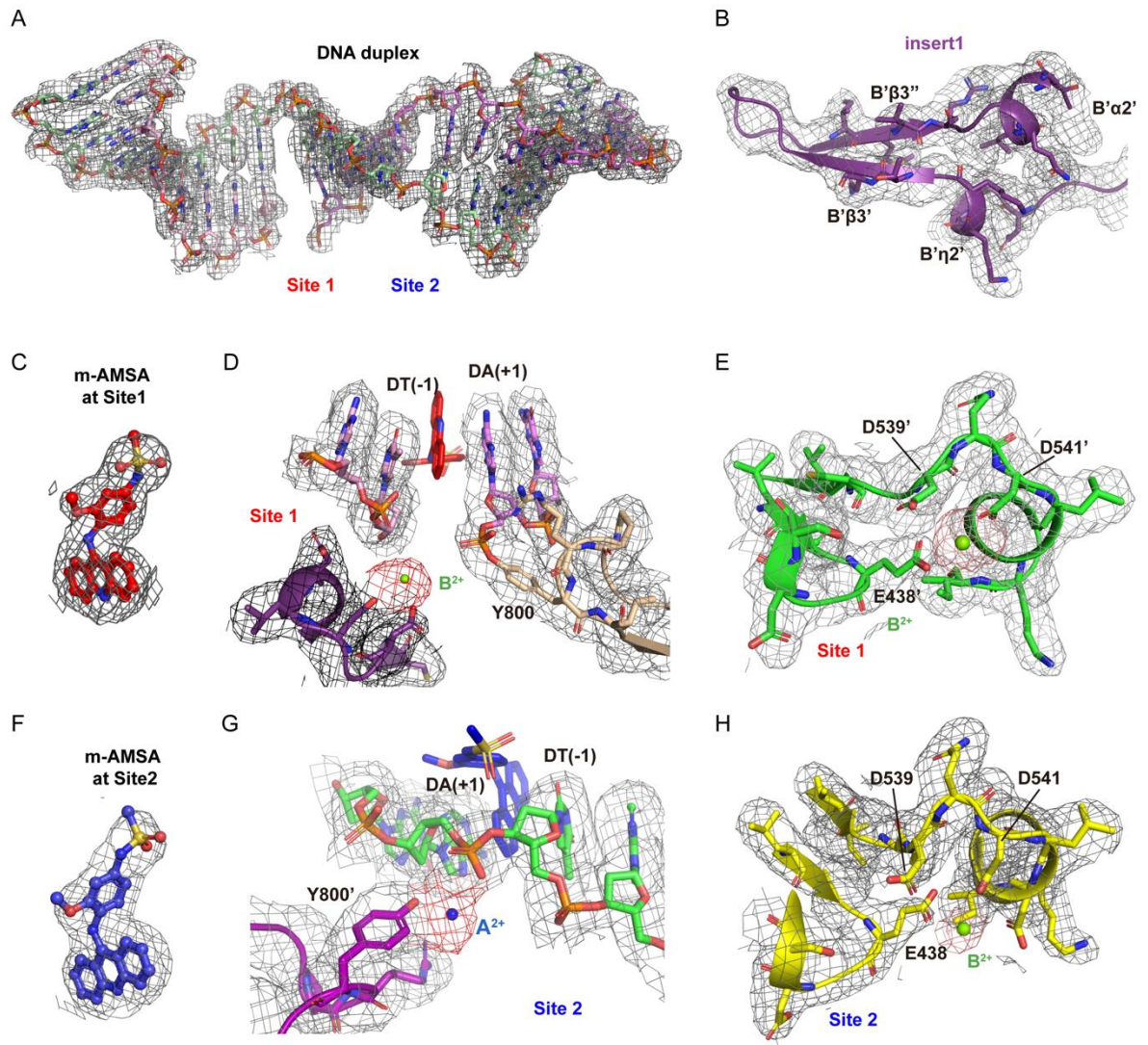
1083 (cyan) and oxidized (orange) forms. The disulfide bond between C72 and C138 has been

1084 highlighted on the right, with residues C72, C138, H73, and D137 in stick presentation. (B)

1085 Cartoon illustrating the dimers of ATPase domain and individual domains of Top IIAs. (C)

1086 Superimposition of ATPase domain monomers in pP1192R (yellow), *S. cerevisiae* Topo II

1087 (pink), and *E.coli* gyrase (cyan). The ATP binding site is indicated by a dashed square. (D)
1088 Structure-based sequence alignment of pP1192R ATPase domain with other Topo IIAs
1089 homologs. Secondary structural elements of pP1192R are indicated above the sequence
1090 alignment. Unique structures in the pP1192R ATPase domain are highlighted.
1091
1092



1093

1094 **Supplementary Fig. 9 Cryo-electron microscopy densities and atomic models of critical**

1095 **structural elements.** (A) EM density for different cleavage states of the DNA duplex. (B) EM

1096 density displays individual beta strands of insert1. (C) EM density around the m-AMSA at Site

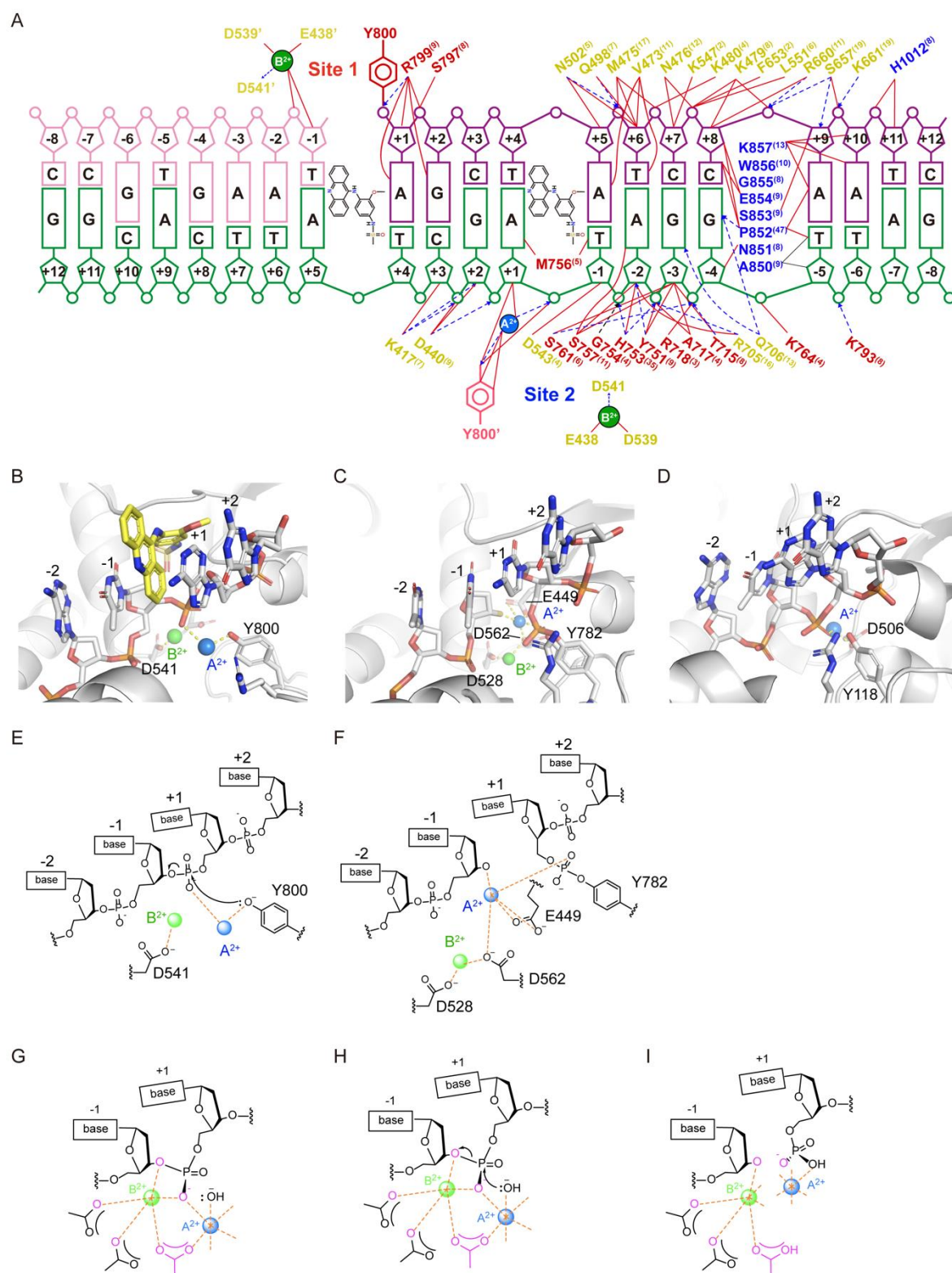
1097 1. (D) Visualization of EM density at cleavage active Site 1, with the +1 nucleotide forming a

1098 phosphotyrosyl linkage with Y800. (E) EM density of the metal ion B^{2+} at Site 1, coordinated

1099 by the metal-binding motif (E...DxD). (F-H) EM density of the m-AMSA (F), the metal ion

1100 A^{2+} (G), and the metal ion B^{2+} together with E...DxD motif (H) at Site 2.

1101



1103

1104 **Supplementary Fig. 10 Detailed interactions between protein, DNA and metal ions. (A)**1105 Schematic of the detailed interactions among the protein, DNA duplex, and Mg^{2+} ions. Red

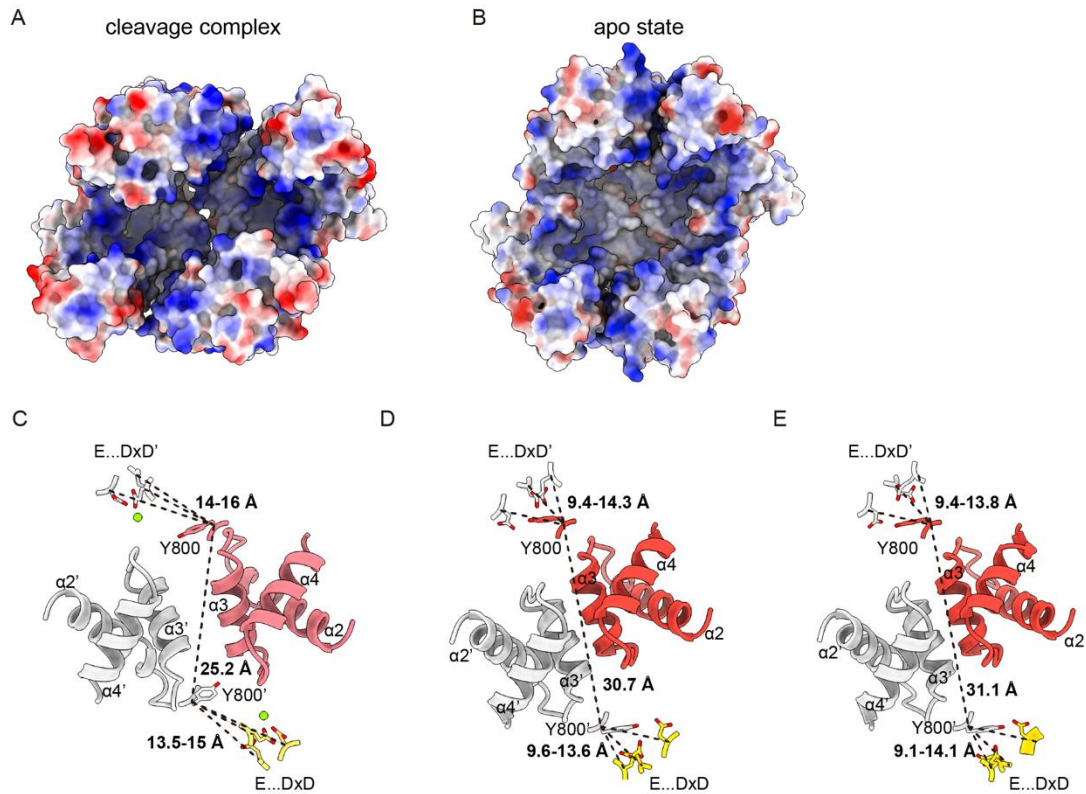
1106 lines highlight all contacts, and the hydrogen bonds or salt bridge interactions are marked by

1107 blue dashed lines. Amino acids in distinct domains are colored as in Fig. 1D. The superscript
1108 number indicates the contacts in which the amino acid is involved, and primes indicate another
1109 protomer. (B-D) Close-up views showing the metal coordination in the pre-cleavage (Site 2 of
1110 the current pP1192R complex) (B), post-cleavage (*S.cerevisiae* Topo II, PDB code 3L4K) (C)
1111 and re-sealed (*S. pneumoniae* Topo IV, PDB code 3KSB) states of Topo IIs. The metal
1112 coordinations are shown as yellow dashed lines. (E and F) Diagrams of the two metal
1113 mechanism in Topo II-mediated DNA cleavage at pre-cleavage (E) and post-cleavage states (F).
1114 (G-I) Model of two metal dependent DNA cleavage at pre-cleavage (G), intermediate-cleavage
1115 (H) and post-cleavage (I) states, $\cdot\bar{O}H$ indicates a deprotonated water molecule or sugar hydroxyl
1116 group that has been activated to become a nucleophile.

1117

1118

1119



1120

1121 **Supplementary Fig. 11 DNA binding-induced conformational changes.** (A and B)

1122 Electrostatic surface presentation of the DNA-binding/cleavage domain in the pP1192R-DNA-

1123 m-AMSA complex (A) and apo structure (B). (C-E) Comparison of the the DNA-binding

1124 groove in different conformations of pP1192R. In each structure, pP1192R-DNA-m-AMSA

1125 complex (C), apo pP1192R in the closed state (D), and apo pP1192R in the open state (E),

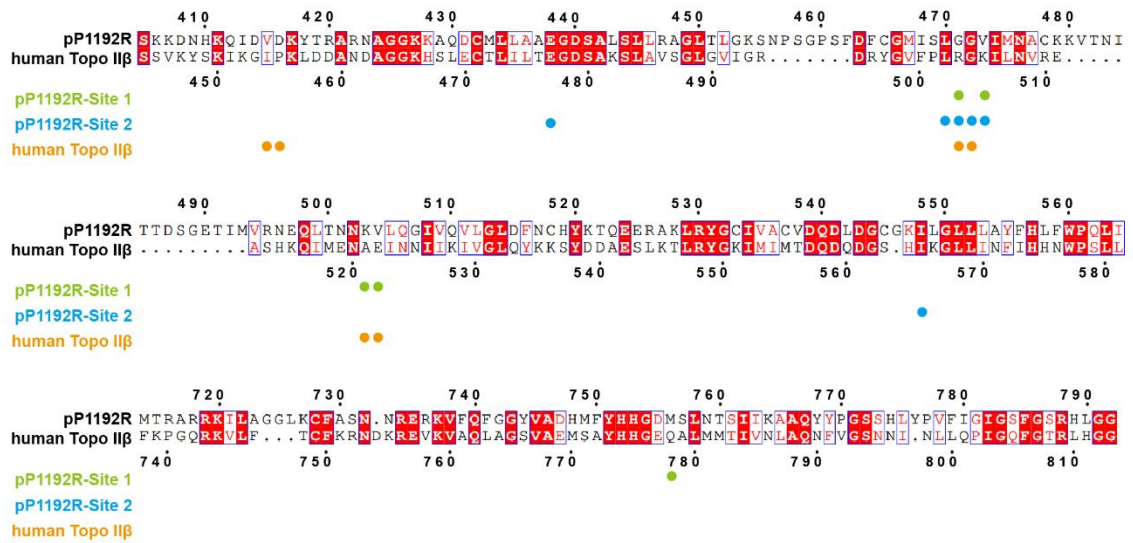
1126 distinguish one monomer with color and the other with gray, labeling the second monomer with

1127 primes. Distances between the two active site tyrosines and between the catalytic tyrosine and

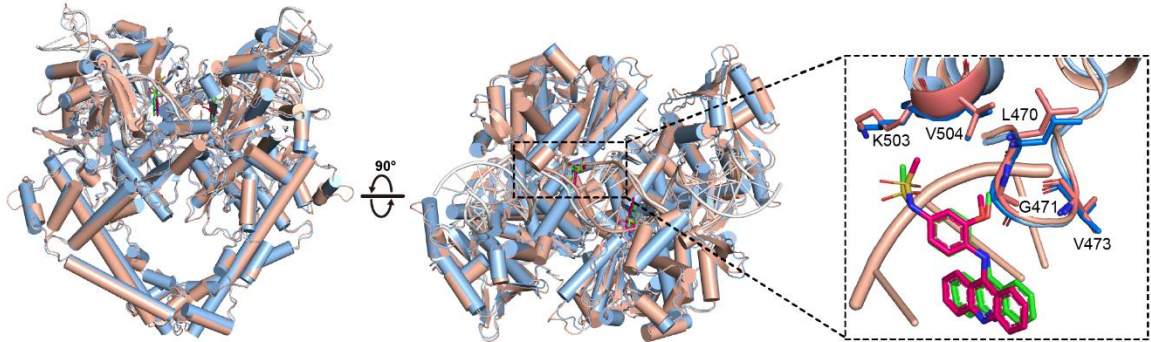
1128 acidic amino acids of the metal-binding motif (E...DxD) are also indicated.

1129

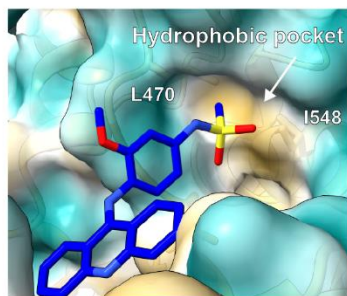
A



B



C



1130

1131 **Supplementary Fig. 12 Structural and sequence analysis of drug binding sites in pP1192R.**

1132 (A) Sequence alignment between pP1192R and human Topo IIβ. Colored spheres below the

1133 sequences highlight amino acids involved in drug interactions at three distinct drug binding

1134 sites. (B) Structural superimposition of the pP1192R-DNA-m-AMSA complex from our study

1135 (pink) and the recently reported one (blue, PDB code: 8J9X), with the m-AMSA binding sites

1136 and the m-AMSAs inside (shown in red for that from our structure and in cyan for that from

1137 8J9X) highlighted. Key residues for drug-protein interaction are shown as sticks and labelled.

1138 (C) Surface representation of drug binding pocket at Site 2.

1139

1140

Table S1. Cryo-EM data collection, refinement and validation statistics

	pP1192R-apo		pP1192R-DNA-m-AMSA complex		
	Open state	Closed state	DNA binding/cleavage domain	Overall-1	Overall-2
EMBD	EMD-39250	EMD-39249	EMD-39245	EMD-39078	EMD-39077
PDB	8YGH	8YGG	8YGE		
Data collection and processing					
Magnification	64	64	105	105	105
Voltage (kV)	300	300	300	300	300
Electron exposure (e-/Å ²)	50	50	50	50	50
Defocus range (µm)	-1.0 ~ -2.0	-1.0 ~ -2.0	-1.0 ~ -2.0	-1.0 ~ -2.0	-1.0 ~ -2.0
Pixel size (Å)	1.08	1.08	0.85	0.85	0.85
Symmetry imposed	C1	C1	C1	C1	C1
Initial particle images (no.)	620,515	620,515	1,957,481	1,957,481	1,957,481
Final particle images (no.)	131,161	78,195	271,076	100,280	170,796
Map resolution (Å)	2.77	2.98	2.76	3.23	3.17
FSC threshold	0.143	0.143	0.143	0.143	0.143
Refinement					
Initial model used (PDB code)	6ZY5	6ZY6	4GFH		
Model resolution range (Å)	Up to 2.77	Up to 2.98	Up to 2.76		
Map sharpening <i>B</i> factor (Å ²)	DeepEMhancer (no <i>B</i> factor value)	DeepEMhancer (no <i>B</i> factor value)	DeepEMhancer (no <i>B</i> factor value)		

Model composition				1142
Non-hydrogen atoms	12246	12102	13479	1143
Protein residues	1510	1490	1558	
Nucleotide	\	\	40	
Ligands	\	\	5	
<i>B</i> factors (Å ²)				
Protein	50.00	50.00	79.14	
Nucleotide	\	\	77.52	
Ligand	\	\	126.72	
R.m.s. deviations				
Bond lengths (Å)	0.004	0.004	0.005	
Bond angles (°)	1.006	0.983	0.598	
Validation				
MolProbity score	2.00	1.89	1.83	
Clashscore	9.85	9.59	6.7	
Poor rotamers (%)	0.00	0.00	1.47	
Ramachandran plot				
Favored (%)	95.67%	97.23%	95.24%	
Allowed (%)	4.33%	2.71%	4.7 %	
Disallowed (%)	0.00%	0.07%	0.06%	

Table S2. Crystallographic data collection and refinement statistics.

pP1192R ATPase domain	
PDB ID code	8YIK
Data collection	
Space group	P6122
Cell dimensions	
<i>a</i> , <i>b</i> , <i>c</i> (Å)	85.75 85.75 211.48
α , β , γ (°)	90.00 90.00 120.00
Wavelength (Å)	0.973
Resolution (Å)	211.5-7.12(1.32-1.30)
<i>R</i> _{merge}	0.092 (1.524)
<i>I</i> / σ <i>I</i>	23.900 (2.300)
CC1/2	1.000 (0.784)
Completeness (%)	98.7 (86.5)
Redundancy	33.4 (14.6)
Refinement	
Limiting resolution (Å)	1.3
No. reflections	111384
<i>R</i> _{work} / <i>R</i> _{free}	0.1871/0.1946
No. atoms	
Protein	3003
Ligand/ion	31
water	414
<i>B</i> -factors	
Protein	18.77
Ligand/ion	11.06
Water	30.51
R.m.s. deviations	
Bond lengths (Å)	0.005
Bond angles (°)	0.758
Ramachandran plot	
Favored (%)	97.61
Allowed (%)	2.39
Outliers (%)	0

*Values in parentheses are for highest-resolution shell.

1 **Table S3. Interactions between DNA duplex, Mg²⁺ ions and pP1192R.**

2

DNA chain C	pP1192R ^{chain/Contacts}	DNA chain D/E	pP1192R ^{chain/Contacts}	Mg ²⁺	pP1192R ^{chain/Contacts}	DNA ^{chain/Contacts}
DG(-8)	/	DC ^D (-8)	/	chain F-1	E438 ^{B/1} , D539 ^{B/1} , D541 ^{B/2}	DT(-1) ^{D/2}
DA(-7)	/	DC ^D (-7)	/	chain F-2	E438 ^{A/1} , D539 ^{A/1} , D541 ^{A/3}	/
DT(-6)	/	DG ^D (-6)	/	chain F-3	Y800 ^{B/3}	DA(+1) ^{C/6}
DT(-5)	K793 ^{A/8} , A850 ^{A/9} , N851 ^{A/3} , P852 ^{A/6}	DT ^D (-5)	/			
DG(-4)	Q706 ^{A/5} , K764 ^{A/4} , N851 ^{A/5} , P852 ^{Aaa/11}	DG ^D (-4)	Q706 ^{B/4} , K764 ^{B/4} , N851 ^{B/10} , P852 ^{B/10}			
DG(-3)	R705 ^{A/2} , Q706 ^{A/8} , T715 ^{A/8} , A717 ^{A/3} , R718 ^{A/3} , Y751 ^{A/1} , S757 ^{A/4} , S761 ^{A/6}	DA ^D (-3)	R705 ^{B/3} , Q706 ^{A/5} , T715 ^{B/6} , A717 ^{B/4} , R718 ^{B/2} , Y751 ^{B/2} , S757 ^{B/4} , S761 ^{B/6}			
DA(-2)	R705 ^{A/14} , A717 ^{A/1} , Y751 ^{A/8} , H753 ^{A/19} , S757 ^{A/7}	DA ^D (-2)	V473 ^{B/1} , D543 ^{B/1} , R705 ^{B/16} , A717 ^{B/1} , Y751 ^{B/7} , H753 ^{B/21} , G754 ^{B/1} , S757 ^{B/7}			
DT(-1)	V473 ^{A/1} , D543 ^{A/4} , H752 ^{A/1} , H753 ^{A/16} , G754 ^{A/4} , M756 ^{A/2}	DT ^D (-1)	E438 ^{B/6} , G472 ^{B/4} , V473 ^{B/6} , D543 ^{B/9} , I548 ^{B/2} , H752 ^{B/1} , H753 ^{B/13} , G754 ^{B/4} , M756 ^{B/2} , S757 ^{B/1}			
DA(+1)	M756 ^{A/3} , Y800 ^{B/6}	DA ^E (+1)	D440 ^{B/1} , M756 ^{B/3} , R799 ^{A/7} , Y800 ^{A/20}			
DG(+2)	K417 ^{A/3} , G439 ^{A/2} , D440 ^{A/8} , Y800 ^{B/1}	DG ^E (+2)	K417 ^{B/1} , D440 ^{B/10} , S797 ^{A/8} , R799 ^{A/2}			
DC(+3)	K417 ^{A/4} , D440 ^{A/1}	DC ^E (+3)	K417 ^{B/2}			
DT(+4)	/	DT ^E (+4)	/			
DA(+5)	N502 ^{B/1}	DA ^E (+5)	V473 ^{A/2} , N502 ^{A/1}			
DT(+6)	V473 ^{B/3} , M475 ^{B/10} , Q498 ^{B/3} , N502 ^{B/5}	DT ^E (+6)	V473 ^{A/9} , M475 ^{A/9} , Q498 ^{A/7} , N502 ^{A/4}			
DT(+7)	V473 ^{B/1} , I474 ^{B/2} , M475 ^{B/10} , N476 ^{B/13} , K479 ^{B/2} , K480 ^{B/1} , K547 ^{B/8}	DC ^E (+7)	I474 ^{A/1} , M475 ^{A/8} , N476 ^{A/4} , K480 ^{A/4} , K547 ^{A/2}			
DC(+8)	N476 ^{B/4} , K479 ^{B/10} , F653 ^{B/1} , K699 ^{B/1}	DC ^E (+8)	N476 ^{A/8} , K479 ^{A/6} , L551 ^{A/1} , F653 ^{A/2} , R660 ^{A/1}			
DC(+8)	P852 ^{B/9} , S853 ^{B/4} , E854 ^{B/12} , G855 ^{B/1}	DC ^E (+8)	Q706 ^{A/1} , P852 ^{A/9} , S853 ^{A/7} , E854 ^{A/9} , G855 ^{A/1}			

DA(+9)	K479 ^{B/1} , S657 ^{B/8} , R660 ^{B/11} , P852 ^{B/15} , S853 ^{B/3} , E854 ^{B/3} , G855 ^{B/6} , W856 ^{B/7} , K857 ^{B/8}	DA ^E (+9)	K479 ^{A/2} , S657 ^{A/15} , R660 ^{A/10} , P852 ^{A/19} , S853 ^{A/2} , G855 ^{A/7} , W856 ^{A/10} , K857 ^{A/9}	
DC(+10)	S657 ^{B/3} , K661 ^{B/3} , K857 ^{B/7} , H1012 ^{B/5} ,	DA ^E (+10)	S657 ^{A/2} , K661 ^{A/3} , K857 ^{A/6} , H1012 ^{A/6}	
DG(+11)	H1010 ^{B/6}	DT ^E (+11)	H1010 ^{A/6} , H1012 ^{A/1}	
DG(+12)	H1010 ^{B/1}	DC ^E (+12)	H1010 ^{A/1}	

3


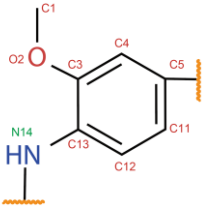
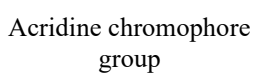
4 *The superscript numbers denote the contacts between pP1192R residues, the DNA duplex, and Mg²⁺ ions, analyzed using the CONTACT program in CCP4
5 suite with a distance cutoff of 4.5 angstroms. Superscript letters specify the chain to which amino acids, nucleotides, and Mg²⁺ belong. Amino acids on chain B
6 are shaded in gray, while those involved in hydrogen bonding or salt bridges, along with nucleotides, are highlighted in red.

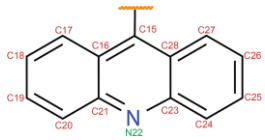
7

8

Table S4. Interaction between AMSA, DNA duplex and pP1192R.

9

m-AMSA		Site 1 pP1192R ^{chain/Contacts}	Site 1 DNA ^{chain/Contact}	Site 2 pP1192R ^{chain/Contacts}	Site 2 DNA ^{chain/Contact}
Methanesulfonamide moiety 	N6	/	/	E438 ^{A/1} , G472 ^{A/4}	DT(-1) ^{C/1} , DA(+1) ^{C/1}
	S7	K503 ^{B/1}	/	E438 ^{A/2} , G472 ^{A/2} , I548 ^{A/1}	DT(-1) ^{C/1}
	C8	K503 ^{B/1} , V504 ^{B/1}	/	E438 ^{A/4} , L470 ^{A/3} , G472 ^{A/2} , I548 ^{A/1}	/
	O9	K503 ^{B/1}	/	G472 ^{A/3} , V473 ^{A/3} , I548 ^{A/1}	DT(-1) ^{C/1}
	O10	K503 ^{B/1} , V504 ^{B/1}	DA(+5) ^{C/1}	E438 ^{A/4} , I548 ^{A/1}	DT(-1) ^{C/3}
Methoxyaniline moiety 	C1	G471 ^{B/2} , V473 ^{B/1}	DA(+5) ^{C/2}	G471 ^{A/3}	DA(+1) ^{C/2} , DG(+2) ^{C/3}
	O2	G471 ^{B/2}	DA(+5) ^{C/4}	G471 ^{A/2}	DA(+1) ^{C/3}
	C3	G471 ^{B/3}	DA(+5) ^{C/2}	G471 ^{A/3} , G472 ^{A/2}	DA(+1) ^{C/2}
	C4	G471 ^{B/1}	/	G471 ^{A/3} , G472 ^{A/2}	DA(+1) ^{C/3}
	C5	/	/	G471 ^{A/1} , G472 ^{A/4}	DT(-1) ^{C/1} , DA(+1) ^{C/1}
	C11	/	DT(+4) ^{C/1}	G472 ^{A/4} , V473 ^{A/1}	DT(-1) ^{C/3}
	C12	G471 ^{B/1}	DT(+4) ^{C/1} , DA(+1) ^{E/3}	G472 ^{A/4} , V473 ^{A/1}	DT(-1) ^{C/3} , DA(+5) ^{E/1}
	C13	G471 ^{B/2}	DA(+1) ^{E/1}	G471 ^{A/2} , G472 ^{A/2}	DT(-1) ^{C/1}
	N14	G471 ^{B/2}	DA(+5) ^{C/3} , DA(+1) ^{E/1}	/	DA(+1) ^{C/1} , DA(+5) ^{E/2}
	C15	/	DA(+5) ^{C/7} , DA(+1) ^{E/3}	/	DA(+1) ^{C/3} , DA(+5) ^{E/4}
Acridine chromophore group 	C16	/	DA(+5) ^{C/4} , DT(-1) ^{D/3} , DA(+1) ^{E/5}	/	DA(+1) ^{C/2} , DT(+4) ^{E/1} , DA(+5) ^{E/7}
	C17	/	DT(-1) ^{D/4} , DA(+1) ^{E/4}	/	DT(+4) ^{E/2} , DA(+5) ^{E/10}



C18	/	DT(-1) ^{D/9} , DA(+1) ^{E/4}	/	DT(+4) ^{E/8} , DA(+5) ^{E/9}
C19	M756 ^{B/2}	DT(-1) ^{D/8} , DA(+1) ^{E/4}	/	DT(+4) ^{E/11} , DA(+5) ^{E/7}
C20	M756 ^{B/2}	DT(-1) ^{D/5} , DA(+1) ^{E/6}	/	DA(+1) ^{C/1} , DT(+4) ^{E/8} , DA(+5) ^{E/7}
C21	/	DA(+5) ^{C/3} , DT(-1) ^{D/3} , DA(+1) ^{E/7}	/	DA(+1) ^{C/4} , DT(+4) ^{E/4} , DA(+5) ^{E/7}
N22	/	DT(+4) ^{C/3} , DA(+5) ^{C/3} , DT(-1) ^{D/1} DA(+1) ^{E/5}	/	DT(-1) ^{C/2} , DA(+1) ^{C/5} , DT(+4) ^{E/3} , DA(+5) ^{E/4}
C23	/	DT(+4) ^{C/4} , DA(+5) ^{C/6} , DA(+1) ^{E/4}	/	DT(-1) ^{C/3} , DA(+1) ^{C/8} , DA(+5) ^{E/3}
C24	/	DT(+4) ^{C/8} , DA(+5) ^{C/5} , DA(+1) ^{E/1}	M756 ^{A/1}	DT(-1) ^{C/5} , DA(+1) ^{C/7}
C25	/	DT(+4) ^{C/10} , DA(+5) ^{C/7}	M756 ^{A/1}	DT(-1) ^{C/8} , DA(+1) ^{C/8}
C26	/	DT(+4) ^{C/10} , DA(+5) ^{C/9}	M756 ^{A/1}	DT(-1) ^{C/8} , DA(+1) ^{C/9}
C27	/	DT(+4) ^{C/4} , DA(+5) ^{C/10}	/	DT(-1) ^{C/6} , DA(+1) ^{C/7}
C28	/	DT(+4) ^{C/3} , DA(+5) ^{C/8} , DA(+1) ^{E/2}	/	DT(-1) ^{C/4} , DA(+1) ^{C/6} , DA(+5) ^{E/3}

10

11

*The superscript numbers denote the contacts between m-AMSA, pP1192R residues, and the DNA duplex, analyzed using the CONTACT program in

12

CCP4 suite with a distance cutoff of 4.5 angstroms. The superscript letters indicate the chain to which the amino acid or nucleotide belongs and the number

13

of contacts in which the amino acid or nucleotide is involved. Amino acids on Chain B are shaded in gray, while those involved in hydrogen bonding or

14

salt bridges, along with nucleotides, are highlighted in red.

15

16

17

18